International Journal on Science and Technology (IJSAT)
E-ISSN: 2229-7677 ● Website: www.ijsat.org ● Email: editor@ijsat.org

Adsorption and Activation of CO_2 on the Surface of Ni_n Clusters (n=2 to 6, 8): An Insight from DFT study

Maksuda Khatun[1], Tanusree Ray[2], Debadrita Roy[1], Nitish Roy[4], and Mahendra Nath Roy[5]

[1,3,4,5]Department of Chemistry, University of North Bengal, Raja Rammahunpur, Darjeeling, W. B., 734013, India;
[2]Department of Chemistry, Siliguri College, Darjeeling, W. B., 734001, India;
[1]maksuda170391@gmail.com; [2]tanusreerayray@gmail.com; [3]debadrita2015@gmail.com;

Abstract:

Here, we have conducted a thorough investigation of the CO_2 activation process on Ni_n clusters (n=2 to 6, 8) using density functional theory. The activation processes and CO_2 adsorption energies are significantly influenced by the clusters that are selected. The number of Ni clusters, the HOMO–LUMO gap, and the charge transfer from cluster to CO_2 molecule all affect the CO_2 activation efficiency. According to our findings, the Ni_4 cluster has a high adsorption energy and, by transferring the charge that can be identified by Mulliken charge analysis, it also considerably alters the bond length and bond angle of the CO_2 molecule. Therefore, Ni_4 and Ni_5 in particular may be useful catalysts for the CO_2 molecule's activation.

Keywords: DFT, CO_2 activation & reduction, Ni_n clusters (n=2 to 6, 8).

Graphical Abstract:

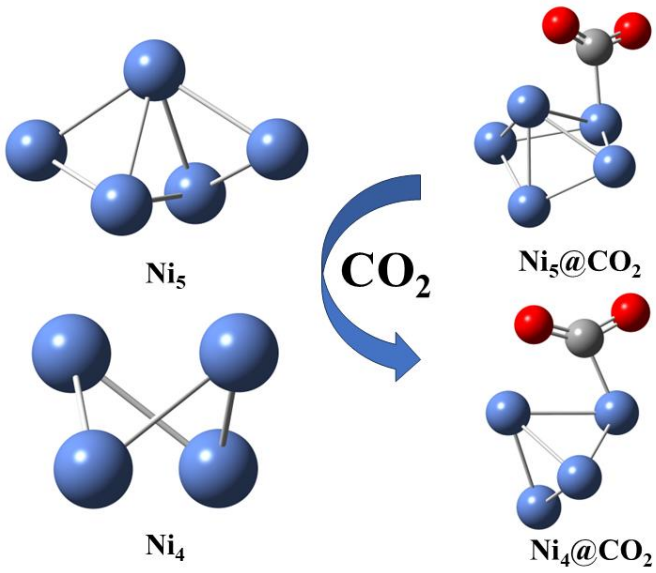

Introduction:

The rapid increase in atmospheric carbon dioxide (CO_2), primarily resulting from the combustion of fossil fuels such as coal, oil, and natural gas, as well as large-scale deforestation, has emerged as one of the most critical challenges of our time [1]. This escalation in CO_2 concentration is a principal driver of climate change and environmental instability, thereby demanding urgent mitigation strategies [2]. One of the most promising approaches lies in the capture, storage, and catalytic conversion of CO_2 into value-added fuels and chemicals. Such a strategy not only addresses greenhouse gas accumulation but also establishes CO_2 as a renewable carbon feedstock for the chemical industry[3, 4].

In this regard, adsorption-based technologies have been extensively explored, employing materials such as metal oxides, zeolites, carbon nanotubes (CNTs), and graphene as adsorbent systems [5]. Both experimental and theoretical studies have demonstrated their potential in efficiently binding CO_2, thereby facilitating subsequent transformation steps. Beyond capture, the catalytic conversion of CO_2 to hydrocarbons is an attractive pathway, with the Sabatier reaction ($CO_2 + 4H_2 \rightarrow CH_4 + 2H_2O$, $\Delta H = -252$ kJ mol^{-1}) serving as a classical example [6]. This route provides not only a sustainable approach to mitigate greenhouse gases but also a practical solution to the global energy crisis, as methane can be directly used as a fuel or feedstock [7]. A crucial step in this conversion process is the adsorption and activation of CO_2. However, the chemical inertness and thermodynamic stability of the linear CO_2 molecule make its activation highly challenging, necessitating the design of efficient catalytic systems [8]. Activation typically requires altering the linear geometry of CO_2 into a bent structure, which substantially lowers the activation energy barrier. It is widely accepted that CO_2 activation on transition metal surfaces is structure-sensitive, with distinct surface geometries influencing reactivity to different extents [9].

Over the years, the catalytic activity of CO_2 on transition metals such as Co, Ni, Cu, Pt, Pd, Fe, and CeO_2 has been extensively studied [10-12]. Results consistently highlight that activation is facilitated through elongation of the C–O bond and increased bending of the O–C–O angle, processes driven by significant electron transfer from the metal surface to the CO_2 molecule [13]. Among these, nickel (Ni) has emerged as one of the most effective catalysts, owing to its ability to stabilize a bent CO_2 intermediate, thereby significantly lowering the reaction barrier [14]. Consequently, Ni-based catalysts have been widely adopted as model systems for unraveling the mechanistic pathways of CO_2 activation and reduction. In this regard, transition metal clusters have attracted considerable attention due to their unique size-dependent electronic, structural, and catalytic properties [15]. Among them, nickel (Ni) clusters are of particular interest because of their moderate cost, abundance, and established role in heterogeneous catalysis, especially in CO_2 hydrogenation and reforming reactions [16]. Unlike bulk Ni surfaces, small Ni_n clusters exhibit distinct geometrical arrangements and discrete energy levels, which often result in enhanced reactivity and tunable catalytic behavior [17].

Density Functional Theory (DFT) has emerged as a powerful computational tool to unravel the adsorption, activation, and conversion mechanisms of CO_2 on metal clusters at the atomic scale [18]. Systematic studies on Ni clusters of varying nuclearity can provide valuable insights into the structure–reactivity relationship, the preferred adsorption geometries, the degree of CO_2 activation, and the underlying electronic factors controlling the process [13].

In this work, we present a comprehensive DFT investigation of CO_2 adsorption and activation on Ni_n clusters (n = 2–6, 8). The chosen cluster sizes represent both small and medium-sized aggregates which exhibits enhanced stability. By analyzing adsorption energies, charge transfer processes, geometrical distortions, and frontier orbital characteristics, this study aims to uncover the role of cluster size in

governing the efficiency of CO_2 activation. The findings provide a fundamental understanding of Ni-based nano-catalysts and may guide the rational design of cluster-supported catalytic systems for CO_2 conversion to value-added products.

2. Methodology:

By using PBEPBE functional analysis, the geometry optimisation of Ni_n clusters (n=2 to 6, 8) and the adsorption of CO_2 molecules on these clusters have been calculated [19]. The Gaussian 09 software suite uses a DFT-based approach [20]. Both metals and non-metals were analysed using the lan2dz basis set [21]. The following formula was used to calculate the adsorption energies (Eads) of $CO_2@Ni_n$ clusters [22].

$$E_{ads} = E_{CO2@Ni} - E_{Ni} - E_{CO2} \quad \ldots\ldots\ldots\ldots\ldots\ldots\ldots\ldots\ldots\ldots(1)$$

Where $E_{CO2@Ni}$ represents the total energy of the CO_2 adsorbed on the Ni_n and E_{Ni}, respectively, and E_{CO2} represents the total energy of the Ni_n and free CO_2. HOMO-LUMO and adsorption energy were among the electro-chemical properties that were evaluated using the same theoretical framework. Furthermore, to understand the magnitude of electron transfer from the Ni_n cluster to CO_2, Mulliken charge & the dipole moment was determined.

Result and Discussion:

1. Geometry and electronic structure of Ni_n (n = 2 to 6, 8) bare clusters

In figure 1, we optimized the structure of Ni_n clusters (n=2 to 6, 8) with the help of PBEPBE functional and lan2dz basis set. Our present work and the previous work are corelated and in table 1, we found that there are similar properties in bond length, bond angle, binding energy and HOMO LUMO band gap [23].

Table 1: Electronic properties of Ni_n clusters

Structure	Ni-Ni bond length (A°)	Binding energy per atom (eV)	HOMO	LUMO	Band gap (eV)	Dipole Moment (D)	Symmetry
Ni_2	Ni1-Ni2= 2.06257	-1.500	-0.177	-0.098	-2.529	0.000	DH
Ni_3	Ni1-Ni2= 2.217 Ni2-Ni3=2.216 Ni1-Ni3=2.216	-2.108	-0.170	-0.069	-2.750	0.0004	CS
Ni_4	Ni1-Ni3=2.249 Ni1-Ni4=2.249 Ni2-Ni4=2.249	-2.268	-0.145	-0.068	-2.099	0.0002	C1

	Ni2-Ni3=2.490						
Ni_5	Ni1-Ni2=2.309 Ni1-Ni3=2.252 Ni2-Ni3=2.302 Ni2-Ni4=2.304 Ni2-Ni5=2.310 Ni4-Ni5=2.252	-2.418	-0.162	-0.089	-1.962	0.442	C1
Ni_6	Ni1-Ni2=2.308 Ni1-Ni3=2.197 Ni2-Ni5=2.235 Ni2-Ni4=2.306 Ni3-Ni5=2.315	-2.531	-0.170	-0.093	-2.100	0.438	C1
Ni_8	Ni1-Ni2=2.397 Ni1-Ni5=2.388 Ni1-Ni3=2.167 Ni1-Ni6=2.410 Ni2-Ni7=2.317 Ni4-Ni5=2.393 Ni5-Ni7=2.408 Ni5-Ni8=2.169 Ni3-Ni6=2.388	-2.761	-0.171	-0.103	-1.867	0.006	C1

	Ni3-Ni8=2.389						

The geometrical parameters of nickel clusters (Ni_2 to Ni_8) reveal interesting size-dependent features. For the dimer Ni_2, the Ni–Ni bond length is found to be 2.06 Å, which is close to reported experimental values. With the growth of cluster size, the Ni–Ni distances increase slightly, lying in the range of 2.21 Å in Ni_3 to around 2.39–2.41 Å in Ni_8, showing structural expansion and relaxation effects in larger aggregates. Particularly, Ni_4 and Ni_5 show bond variations from 2.25 Å to 2.49 Å, highlighting distorted geometries in intermediate sizes.

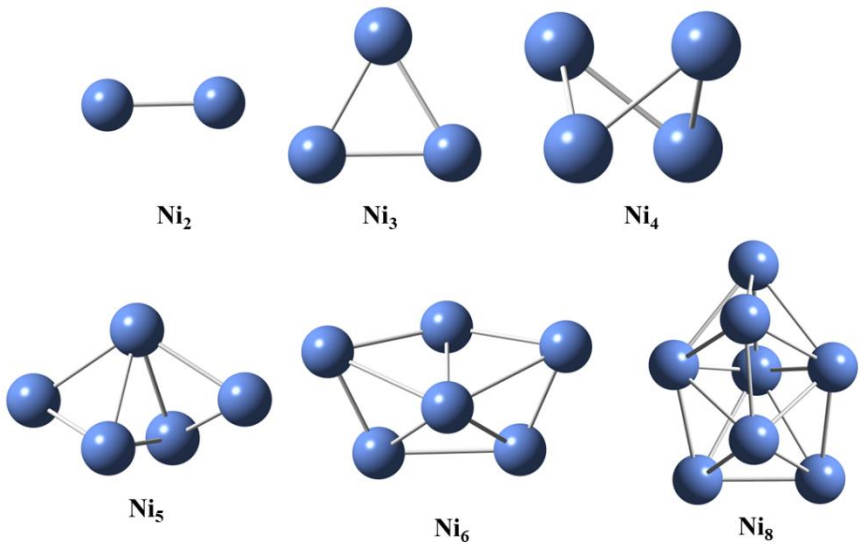

Figure 1. Optimized structures of Ni_n clusters (n=2 to 6, 8) with DFT

Furthermore, to investigate the thermodynamic stability we calculated the binding energy per atom (ΔE_b) by using Equation (2).

$$\Delta E_b = \frac{[E_{(Ni_n)} - n\, E_{Ni}]}{n} \quad \ldots\ldots\ldots\ldots\ldots\ldots\ldots\ldots\ldots\ldots (2)$$

where, n is the number of Ni atoms; $E_{(Ni_n)}$ is the total energy of Ni clusters and E_{Ni} is the energy of an isolated Ni atom, respectively [24]. The negative binding energy estimates show that the Ni_n clusters are thermally stable. The binding energy per atom increases steadily with cluster size, reflecting enhanced stability. Ni_2 has the least stable configuration with a binding energy of –1.500 eV, while stability improves significantly for larger clusters, reaching –2.761 eV for Ni_8. This trend suggests that nickel clusters become thermodynamically more stable as the nuclearity increases, in line with the general trend observed for transition metal clusters.

In figure 2, the energies of the highest occupied molecular orbital (HOMO) and lowest unoccupied molecular orbital (LUMO) indicate the electronic properties of the clusters. Ni_2 shows a HOMO energy

of –0.177 eV and a LUMO energy of –0.098 eV. As cluster size increases, the LUMO shifts gradually, while HOMO values remain in a narrow energy window. These changes reflect the redistribution of electronic density with increasing cluster size. The HOMO–LUMO gap exhibits notable variations across the clusters. For Ni_2, the gap is –2.529 eV, which slightly increases to –2.750 eV in Ni_3, indicating greater electronic stability. However, from Ni_4 onwards, the band gap decreases, reaching as low as –1.867 eV in Ni_8. This reduction points to increasing metallic character and improved electronic conductivity with higher cluster sizes, which is crucial for catalytic applications.

The dipole moment provides further insight into the polarity and charge distribution of the clusters. Ni_2 and Ni_3, with higher symmetry (DH and CS), show negligible dipole values (~0.000 D). In contrast, distorted geometries such as Ni_5 and Ni_6 exhibit significant dipole moments around 0.44 D, signifying asymmetric charge distributions. Interestingly, Ni_8 returns to near-zero dipole values, consistent with its more compact and stable structure. Cluster symmetry evolves as the size increases. Ni_2 shows DH symmetry, while Ni_3 exhibits CS symmetry, both representing relatively ordered structures. From Ni_4 onwards, clusters primarily adopt C_1 symmetry, which is associated with distortions and asymmetry, reflecting the structural flexibility required to minimize overall energy. This reduction in symmetry often correlates with increased reactivity.

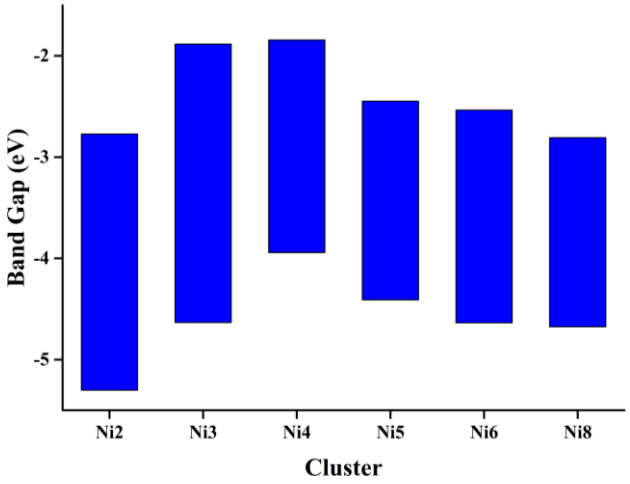

Figure 2. Band gap and HOMO LUMO levels of the Ni_n clusters

3.2. Adsorption and Activation of CO_2 on Ni_n Clusters (n=2 to 6, 8):

Our main objective is to examine the adsorption and activation of CO_2 molecules on various sized Ni clusters following the optimisation of Ni_n clusters (n=2 to 6, 8). In order to do this, we consider the lowest energy structure of bare Ni clusters (as illustrated in Figure 1). The adsorption energy (E_{ads}), which measures the interaction between the CO_2 molecule and the clusters, is found using equation 1. With the exception of Ni_2, all systems are deemed acceptable for CO_2 adsorption based on the negative adsorption energy. Figure 3 depicts the adsorption energy diagram. Remarkably, the majority of the Ni clusters exhibited CO_2 activation, as seen in figure 4. Ni_4 has the highest Eads, whereas Ni_3 has the lowest.

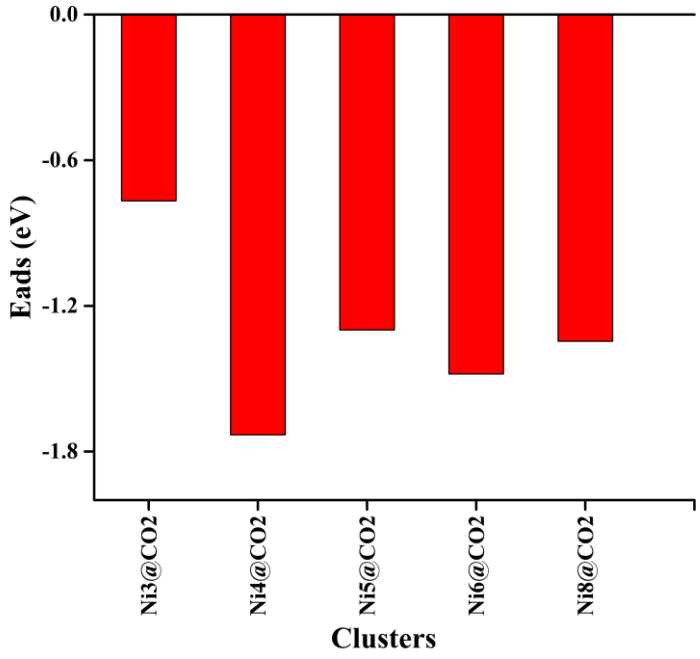

Figure 3. Variation of adsorption energy (E_{ads}) of CO_2 on Ni_n Clusters (n=2 to 6, 8)

The optimized lowest energy structures of Ni_n clusters (n = 2–6, 8) interacting with CO_2 molecules, obtained using the PBEPBE functional, are presented in Figure 4. It can be clearly observed that the CO_2 molecule preferentially adsorbs at the triangular face of these nickel clusters. This adsorption geometry remains consistent across the different cluster sizes studied. The interaction results in the formation of Ni–C bonds, which serve as key indicators of CO_2 activation. Interestingly, the bond lengths of Ni–C vary depending on the cluster size and geometry, reflecting the size-dependent reactivity of the clusters. Thus, the adsorption pattern highlights the unique structural and electronic features of small Ni clusters in promoting CO_2 activation.

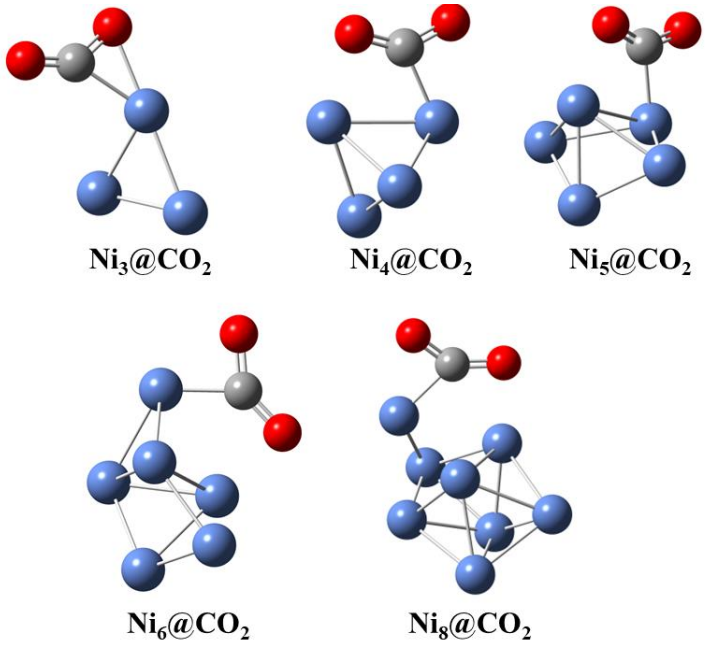

Figure 4. Optimized structures of CO_2@Ti_n clusters

Further analysis of Table 2 revealed that all the clusters are able to adsorb and activate the CO_2 molecule strongly with the very large change or elongation of the C-O bond lengths (d_{C-O}) in comparison to the corresponding length in a free CO_2 molecule. There is an increase of around 0.08Å in the C-O bond length for most of the clusters as compared to that of bare CO_2 (1.16 Å). The maximum elongation of C-O bond length of 0.17 Å is observed when the CO_2 molecule gets adsorbed on $Ni_8@CO_2$ cluster. During this activation process of CO_2 on the Ni clusters, there is a formation of Ni-C bond with the average bond length of 1.8 Å.

A detailed examination of Table 2 clearly demonstrates that all the investigated nickel clusters exhibit a strong ability to adsorb and activate the CO_2 molecule. This activation is evident from the significant elongation of the C–O bond lengths (d_{C-O}) compared to the corresponding values in free CO_2. In its isolated state, the C–O bond length of CO_2 is about 1.16 Å, serving as the reference for comparison. Upon adsorption onto the Ni clusters, the C–O bonds undergo noticeable changes, confirming the weakening of the intramolecular bonds and the onset of activation. For most of the clusters studied, an elongation of approximately 0.08 Å in the C–O bond length is observed relative to free CO_2. This elongation highlights the influence of the Ni surface in destabilizing the linear CO_2 structure. The effect becomes even more pronounced for larger clusters, particularly the $Ni_8@CO_2$ complex, where the maximum C–O bond elongation of 0.17 Å is recorded. Such a considerable bond extension indicates a stronger interaction between CO_2 and the Ni cluster surface, thereby facilitating the activation process. Alongside this elongation, the adsorption process also induces the formation of a Ni–C bond, further stabilizing the CO_2 molecule on the cluster. The average bond length of this newly formed Ni–C interaction is calculated to be around 1.8 Å. This dual feature of C–O bond elongation and Ni–C bond formation strongly supports the conclusion that nickel clusters can efficiently promote CO_2 activation. Thus, the structural changes observed provide direct evidence of the potential of Ni_n clusters as effective nanocatalysts for CO_2 activation.

Table 2: Calculation of C-O and Ni-C Bond length of CO_2 on Ni_n Clusters (n=2 to 6, 8) clusters

Cluster Systems	**C-O Bond length (Å) in CO_2**	**Ni-C Bond length (Å) in $CO_2@Ni_n$**
$Ni_3@CO_2$	1.242	1.880
$Ni_4@CO_2$	1.232	1.779
$Ni_5@CO_2$	1.250	1.790
$Ni_6@CO_2$	1.235	1.780
$Ni_8@CO_2$	1.337	1.792

A crucial observation from the structural analysis is the variation in the O–C–O bond angles of CO_2 upon adsorption onto the Ni_n clusters, as depicted in Figure 5. In its free state, the CO_2 molecule possesses a linear geometry with a bond angle of 180°. However, once chemisorbed on the nickel clusters, this angle undergoes a substantial reduction, falling within the range of 148° to 139°. Such a distortion corresponds to a decrease of approximately 32° to 41° relative to the bare CO_2 molecule.

This pronounced bending of the O–C–O angle provides direct evidence of strong interaction between CO_2 and the cluster surface, highlighting the ability of Ni clusters to activate the otherwise stable and inert CO_2 molecule. The deviation from linearity is a well-established indicator of activation, as it reflects the weakening of π bonds within the CO_2 framework and enhanced charge transfer from the metal cluster to the antibonding orbitals of CO_2.

Notably, the most significant changes in bond angle are observed in the Ni_4 and Ni_5 clusters, suggesting that medium-sized clusters are particularly effective in facilitating the activation process. These findings, in conjunction with the elongation of the C–O bonds and formation of Ni–C bonds, conclusively demonstrate that Ni_n clusters serve as efficient nanostructured platforms for CO_2 adsorption and activation.

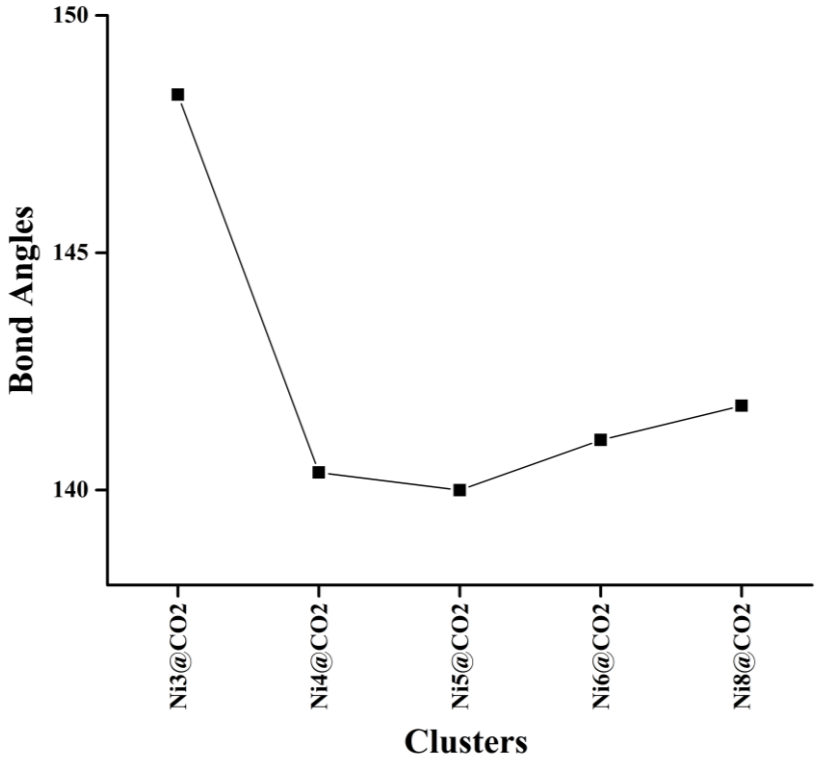

Figure 5. Change of the bond angle of CO_2 on CO_2@Ni_n Clusters (n=2 to 6, 8)

3.3. Mulliken charge analysis of the CO_2 activated clusters:

It is well established that the activation of CO_2 is strongly facilitated by the transfer of electronic charge from the transition metal surface to the lowest unoccupied molecular orbital (LUMO) of the CO_2 molecule [25]. Such charge transfer weakens the C–O bonds and bends the linear geometry, thereby enhancing reactivity. In this context, we carried out a systematic investigation of the charge transfer between the selected Ni_n clusters and the adsorbed CO_2 molecule to elucidate the underlying mechanism of activation. To quantify this effect, Mulliken charge analysis was performed on each cluster–CO_2 complex. The results, presented in Figure 6, clearly indicate that the net negative charge accumulated on the chemisorbed CO_2 molecule lies in the range of –0.2435e to –0.30027e. Among the studied systems, the Ni_6@CO_2 complex exhibits the largest degree of charge transfer, with a net charge of –0.30027e on CO_2. This finding is consistent with the significant elongation of the C–O bond observed in Ni_6@CO_2 relative to free CO_2, highlighting the strong correlation between charge transfer and bond activation. Furthermore, a general trend is observed across the cluster series: as the net negative charge on the chemisorbed CO_2 molecule increases, the C–O bonds undergo greater elongation. This direct relationship reinforces the conclusion that charge donation from the Ni clusters into the antibonding orbitals of CO_2 is the primary driving force behind its activation.

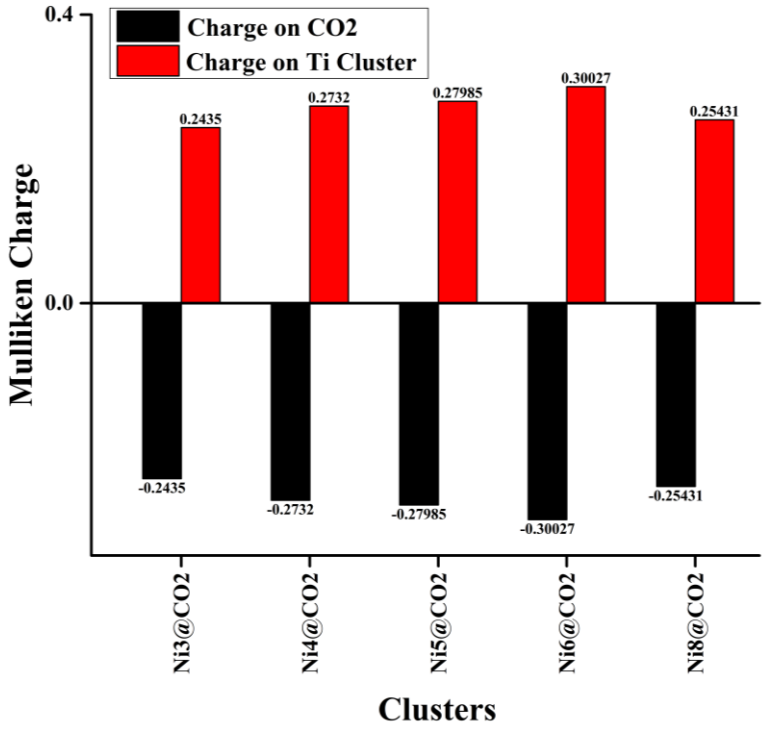

Figure 6. Mulliken charge on CO_2 and Ni clusters of Ni_n and $CO_2@Ni_n$ Clusters (n=2 to 6, 8) clusters

4. Conclusion

In the present study, we have carried out a comprehensive investigation of CO_2 adsorption and activation on Ni_n clusters (n = 2–6, 8) with the ultimate objective of understanding their potential in the reduction of CO_2 to value-added fuels such as methane. The interaction of CO_2 with these clusters plays a crucial role in modulating their electronic structures, which in turn governs the adsorption energies and activation mechanisms. Our findings reveal that the efficiency of CO_2 activation is highly dependent on the cluster size, the electronic band gap, and the extent of charge transfer from the metal cluster to the CO_2 molecule. Notably, the Ni_3 cluster displays relatively low adsorption energy, indicating weaker CO_2 binding, whereas the Ni_4 cluster demonstrates significantly higher adsorption energy, accompanied by substantial charge transfer to CO_2. This enhanced charge transfer not only strengthens the interaction but also results in remarkable modifications in the C–O bond lengths and the O–C–O bond angle of the chemisorbed CO_2 molecule. Among the examined systems, the Ni_4 cluster stands out as the most effective, as it induces pronounced structural distortions in CO_2, thereby facilitating a high degree of activation. These results clearly demonstrate that the Ni_4 cluster plays a pivotal role in enhancing CO_2 reactivity through efficient charge donation, establishing it as a promising candidate for catalytic CO_2 reduction.

Financial support

The authors acknowledge no financial support from any funding resources.

Declaration of competing interest

The authors declare that they have no known competing financial interests or personal relationships that could have appeared to influence the work reported in this paper.

Acknowledgements: The authors are grateful to Gour Mahavidyalaya, Malda-732142, India for providing computational resources support in order to continue this research work.

Author Contributions Statement:

Maksuda Khatuna: Computational Work, Drafting of manuscript, Original Research.

Tanusree Ray: Drafting of manuscript, Original Research.

Debadrita Roy:
Nitish Roy: Supervision, Drafting, Original Research.
Mahendra Nath Roy: Drafting of manuscript, Original Research, Supervision.

References:

1. R. Dhillon, G. von Wuehlisch, Mitigation of global warming through renewable biomass, Biomass and bioenergy, 48 (2013) 75-89.
2. L.J. Nunes, The rising threat of atmospheric CO_2: a review on the causes, impacts, and mitigation strategies, Environments, 10 (2023) 66.
3. O. Awogbemi, D.A. Desai, Novel technologies for CO_2 conversion to renewable fuels, chemicals, and value-added products, Discover nano, 20 (2025) 29.
4. D.C. Makepa, C.H. Chihobo, Sustainable pathways for biomass production and utilization in carbon capture and storage—a review, Biomass Conversion and Biorefinery, 15 (2025) 11397-11419.
5. S. Satyam, S. Patra, Innovations and challenges in adsorption-based wastewater remediation: A comprehensive review, Heliyon, 10 (2024).
6. G. Varvoutis, Design and evaluation of advanced CeO_2-based transition metal catalytic composites for CO_2 activation by renewable H_2 toward synthetic CH_4 and CO, in, Πανεπιστήμιο Δυτικής Μακεδονίας. Σχολή Πολυτεχνική. Τμήμα Μηχανολόγων Μηχανικών, 2022.
7. S. Singh, Energy crisis and climate change: Global concerns and their solutions, Energy: crises, challenges and solutions, (2021) 1-17.
8. C. Song, Global challenges and strategies for control, conversion and utilization of CO_2 for sustainable development involving energy, catalysis, adsorption and chemical processing, Catalysis today, 115 (2006) 2-32.
9. D. Cheng, K.-L.C. Nguyen, V. Sumaria, Z. Wei, Z. Zhang, W. Gee, Y. Li, C.G. Morales-Guio, M. Heyde, B. Roldan Cuenya, Structure sensitivity and catalyst restructuring for CO_2 electro-reduction on copper, Nature Communications, 16 (2025) 4064.
10. M. Konsolakis, M. Lykaki, Facet-dependent reactivity of ceria nanoparticles exemplified by CeO_2-based transition metal catalysts: A critical review, Catalysts, 11 (2021) 452.
11. C. Liu, T.R. Cundari, A.K. Wilson, CO_2 reduction on transition metal (Fe, Co, Ni, and Cu) surfaces: In comparison with homogeneous catalysis, The Journal of Physical Chemistry C, 116 (2012) 5681-5688.
12. A. Temitope, Advances in heterogeneous catalysts for hydrogen production, (2025).
13. U.J. Etim, C. Zhang, Z. Zhong, Impacts of the catalyst structures on CO_2 activation on catalyst surfaces, Nanomaterials, 11 (2021) 3265.
14. L. Shen, J. Xu, M. Zhu, Y.-F. Han, Essential role of the support for nickel-based CO_2 methanation catalysts, Acs Catalysis, 10 (2020) 14581-14591.
15. J. Alonso, Electronic and atomic structure, and magnetism of transition-metal clusters, Chemical reviews, 100 (2000) 637-678.
16. S. De, J. Zhang, R. Luque, N. Yan, Ni-based bimetallic heterogeneous catalysts for energy and environmental applications, Energy & environmental science, 9 (2016) 3314-3347.
17. J. Niu, C. Zhang, H. Liu, Y. Jin, R. Zhang, J. Ran, Unraveling the effects of Ni particle size and facet on CH_4 activation: From cluster to nanoparticle, International Journal of Hydrogen Energy, 48 (2023) 19486-19493.

18. Á. Morales-García, F. Vines, J.R. Gomes, F. Illas, Concepts, models, and methods in computational heterogeneous catalysis illustrated through CO_2 conversion, Wiley Interdisciplinary Reviews: Computational Molecular Science, 11 (2021) e1530.
19. G.A. Cisneros, M. Castro, D.R. Salahub, DFT study of the structural and electronic properties of small Ni_n (n= 2–4) clusters, International journal of quantum chemistry, 75 (1999) 847-861.
20. S.M. Putra, T.K. Wungu, I. Arif, Ab-Initio Calculation of Chlorophyll-b UV-Vis Absorbance Spectra using Gaussian 09 based Density Functional Theory (DFT), International Journal of Nanoelectronics & Materials, 14 (2021) 11-26.
21. B. Ali, Q.U. Ain, M. Azeem, Z. Lin, Tuning Graphitic Carbon Nitride: A Computational Study of Metal, Semiconductor, and Non-Metal Doping Effects on Electronic and Thermodynamic Properties, Journal of Physics and Chemistry of Solids, (2025) 112878.
22. K. Ghosh, N.K. Mridha, A.A. Khan, N. Baildya, T. Dutta, K. Biswas, N.N. Ghosh, CO_2 activation on transition metal decorated graphene quantum dots: An insight from first principles, Physica E: Low-dimensional Systems and Nanostructures, 135 (2022) 114993.
23. F. Reuse, S. Khanna, Geometry, electronic structure, and magnetism of small Ni_n (n= 2–6, 8, 13) clusters, Chemical physics letters, 234 (1995) 77-81.
24. V. Grigoryan, M. Springborg, A theoretical study of the structure of Ni clusters (Ni N), Physical Chemistry Chemical Physics, 3 (2001) 5135-5139.
25. O. Mohan, Q.T. Trinh, A. Banerjee, S.H. Mushrif, Predicting CO_2 adsorption and reactivity on transition metal surfaces using popular density functional theory methods, Molecular Simulation, 45 (2019) 1163-1172.